Centrifuge modeling of seismic settlement of composite breakwaters

Modélisation expérimentale du tassement sismique du sol de digue à l'aide du test centrifuge

K.Kita – *Department of Marine Civil Engineering, Tokai University, Shizuoka, Japan*
H.Yamada – *Graduate School of Civil Engineering, Kyoto University, Japan*

ABSTRACT: In the 1995 Hyogoken-Nambu earthquake, some composite breakwaters in Kobe port experienced over 2.5m settlement. Although the importance of undrained cumulative shear deformation in foundation ground was pointed out as a possible mechanism of breakwater settlement due to strong shaking, a full understanding of the mechanism has not yet been reached. In this study, a series of shaking table tests were conducted on composite breakwater systems, aiming at clearly understanding the nature of seismic settlement due to undrained shear deformation of foundation ground, as well as the nature of seismic settlement due to penetration of mound rubbles into foundation soil. A high-speed CCD camera (250 frames/sec.) was introduced to observe the seismic behavior of a caisson model, rubble mound and underlying soil during earthquake shaking.

RÉSUMÉ: Lors du tremblement de terre à Hyogoken-Nambu en 1995, quelques digues composites du port de Kobe ont accusé un tassement de plus 2.5 m. Bien que l'importance de la déformation de cisaillement cumulée et non-drainée ait été désignée comme un mécanisme possible du tassement de la digue dû aux fortes secousses, une compréhension complète du mécanisme n'a pas été encore obtenue. Dans cette étude, une série d'essais à la table à choc a été effectuée sur des digues composites, avec pour objectif de clarifier la nature du tassement sismique dû à la déformation de cisaillement non-drainée du sol de fondation ainsi que la nature du tassement sismique dû à la pénétration de massifs d'enrochements dans le sol de fondation. Un appareil photo à grande vitesse (CCD, 250 photos/seconde) a récemment été utilisé afin d'observer le comportement sismique d'un caisson modèle, du massif d'enrochements et du sol sous-jacent durant les secousses du tremblement de terre.

1 INTRODUCTION

Composite breakwaters in the port of Kobe underwent large settlements over 2.5m during the 1995 Hyogoken-Nambu earthquake. Sekiguchi et al. (1996a) carried out underwater acoustical surveying around breakwaters No. 6 South and No. 7 in the port of Kobe in order to investigate the mechanism that caused the large settlements and observed following features; (1) breakwaters settled almost uniformly along their longitudinal axes and settlement of the crest of the rubble mound near the caisson wall was generally larger than that on the shoulder, and (2) some features of sand boil were found in the open area of the foundation sand fill, implying the occurrence of liquefaction. It was however noted that the foundation soils just beneath the main part of the breakwater should have remained stable against liquefaction due to the state of anisotropic stress induced by the weight of the caisson and rubble mound (Iai et al., 1998). Sekiguchi et al. (1996b) suggested the undrained cumulative shear deformation as the key mechanism of large deformation of foundation soils, based on the results of cyclic torsional shear tests on saturated fine silica sand.

Another possible mechanism responsible for the large settlements of breakwater could be inspired from the dynamic centrifuge tests on gravel embankments by Peiris et al. (1998). They observed failure of gravel embankments associated with penetration and scattering of gravel into the foundation ground. However, here remained unknown the effect of dispersion of coarse particles on the settlement of composite breakwaters.

In this study, a series of shaking table tests were conducted on composite breakwater systems in a centrifuge, with the aim of clarifying the nature of the seismic settlement due to the undrained shear deformation of foundation ground and the dispersion of mound rubbles into foundation soil

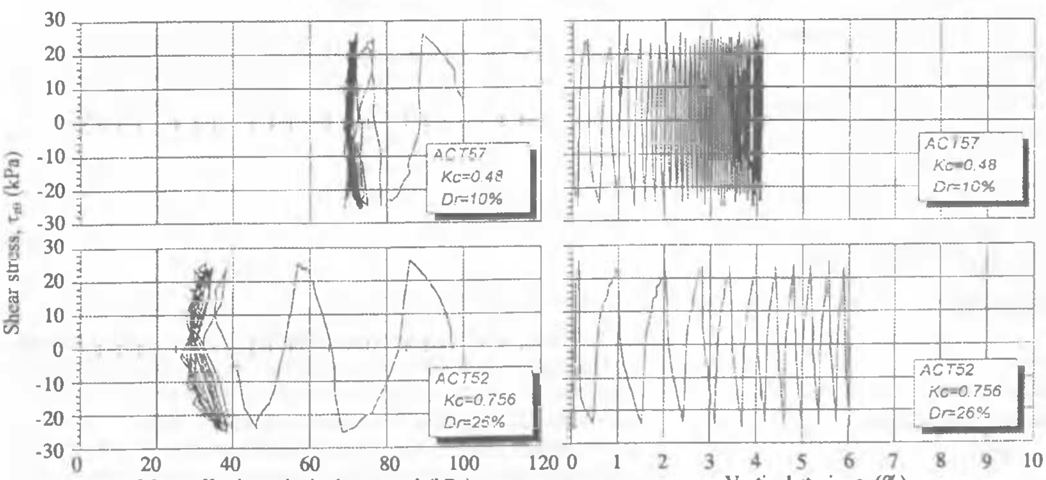

Figure 1. Effective stress paths and relationships between shear stress and strain obtained from cyclic torsional shear tests (Tanaka, 1996).

2 MECHANISM OF UNDRAINED CUMULATIVE SHEAR DEFORMATION OF FOUNDATION GROUND BENEATH BREAKWATERS

Undrained cyclic torsional shear tests have been conducted by Tanaka (1996) on two saturated sand specimens in loose states (Dr=10% and 26%) with different initial anisotropic consolidation stress ratios ($K_c=\sigma_{ho}'/\sigma_{vo}'$=0.48 and 0.756). Effective stress paths and relationships between shear stress and vertical strain are shown in Figure 1. These figures reveal that; (1) effective stress paths cross Phase Transformation Lines (PTLs) at certain positive values of effective confining stress, and the effective confining stresses do not decrease significantly afterwards. (2) Vertical compressive strains develop drastically due to cyclic shearing after the stress paths reach PTLs. In fact, this vertical compression of sand specimen was accompanied by the horizontal extension under the undrained condition. (3) The larger the consolidation stress ratio, the smaller the effective confining stress at phase transformation is, introducing larger axial strain due to cyclic loading after the phase transformation. The above-mentioned results suggest the importance of initial shear stress on the dynamic deformation behavior of sandy soils under undrained conditions.

Figure 2 shows a distribution of initial shear stress ratio induced by self-weights of caisson, rubble mound and foundation soils, which is calculated in view of the configurations of break-

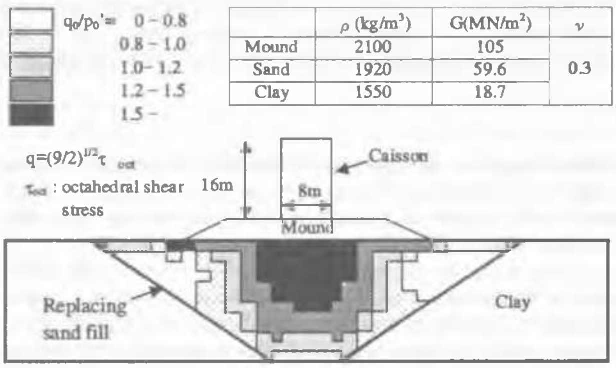

Figure 2. Distribution of initial shear stress ratio in foundation ground beneath breakwater by plane strain analysis.

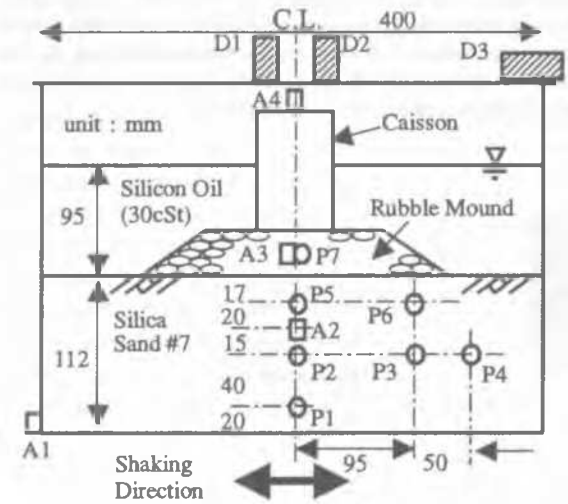

A1 - A4 : Accelerometers
P1 - P7 : Pore Pressure Transducers
D1 - D3 : Laser Displacement Transducers

Figure 3. Experimental setup.

water No. 6 South in Kobe Port. It can be seen that large stress ratios are introduced at the shallow depths of the foundation ground just beneath the caisson and rubble mound. In conjunction with what was observed in the cyclic torsional shear tests, foundation soils in this region should have low liquefaction potential. However, once the effective stress path reaches PTL, the undrained cumulative shear deformation mechanism would become operational, causing large compression in vertical direction together with the horizontal extension. It should also be noted here that the initial stress ratio decreases with depth beneath the main part of the composite breakwater.

3 CENTRIFUGAL SHAKING TABLE TESTS

3.1 *Test procedures*

Shaking table tests were performed under a centrifugal acceleration of 30 gravities. Typical configuration of breakwater-foundation ground model is depicted in Figure 3. Test conditions and the observed settlements are summarized in Table 1.

A spoonful of fine silica sand (D=0.1mm, G_s =2.68) was sprinkled over de-aired silicon oil, forming horizontal foundation deposits. Silicon oil with the viscosity of 30cSt was used as submerging fluid as well as pore fluid, for the purpose of matching time scalings of vibration and consolidation in dynamic centrifuge tests. Colored sand was spotted and lined in the foundation ground to facilitate deformation measurements. After consolidation of the foundation ground under 30g centrifugal conditions, a trapezoidal mound was formed using gravel (D=4.76-9.5mm, G_s=2.71) or coarse silica sand (D=0.85-2mm, G_s=2.64). A rectangular model caisson (height=100mm, width=60mm, breadth=100mm, mass=1.42kg) was then placed on the mound. Pore pressure transducers and horizontal accelerometers were installed in the foundation ground and the mound. Three laser displacement transducers were used to measure the caisson displacements.

Each model was subjected to 20 cycles of horizontal sinusoidal excitation at 30 Hz, with the acceleration amplitude of approximately 5 gravities (cases 1 to 7) or 7 gravities (cases 8 and 9). A high-speed CCD camera was instrumented for visual observation of the seismic behavior of caisson, rubble mound and underlying soil deposits during shaking. Pictures were recorded at a rate of 250 frames/sec with a resolution of 640 by 480 pixels. The recording duration was 3.256 seconds.

Table 1 Summary of experiments

Case No.	Foundation ground Dr (%)	Mound Materials	Caisson settlement (mm)	Penetration ratio of mound (%)
1	47	Gravel	15	23
2	44	Silica sand	17	8
3	31	Gravel	26	21
4	15	Gravel	55	16
5	30	Silica sand	35	4
6	58	Gravel*	16	21
7	37	Gravel	34	19
8	22	Gravel	38	24
9	23	Silica sand	39	4

*Particle size : 9.5mm<D

3.2 *Results and discussion*

Time histories of horizontal accelerations, excess pore pressures and caisson settlement measured in case 8 are shown in Figure 4. The relative density of the foundation ground was 22% and the amplitude of the shaking acceleration was 7 gravities.

Amplitude of ground acceleration measured with accelerometer A2 attenuates to about 50% of that of base acceleration (A1) from the early stage of earthquake loading, implying the immediate softening of soils in the lower part of the foundation ground. This may conform to the excess pore pressure response measured at the deep part of the foundation ground beneath the caisson and mound (P1). The residual pore pressure developed markedly to 50kPa during the first several cycles of shaking, which is the same level as the initial effective vertical stress at the location estimated by the elasticity theory (σ_{vo}'=45kPa). Frequency of pore pressure fluctuation at P1 doubles the loading frequency, indicating the cyclic mobilization of effective confining stress. Accelerations in the mound (A3) and at the caisson top (A4) are slightly amplified relative to ground acceleration. Excess pore pressure at the middle and shallow depths of foundation ground (P2 and P5) take negative values first, then increase to positive values partly due to the settlement of transducers. The residual pore pressures are smaller than the initial effective vertical stresses at these locations.

Excess pore pressure measured at the middle depth of foundation ground beneath the open area (P4) attained 20kPa after a few cycles of loading. Initial effective vertical stress at P4 is 19.5kPa, therefore the soils would undergo liquefaction in the shallow part of the foundation ground below the open area. This may lead to the reduction of horizontal effective confining stress onto the soils beneath the caisson and mound, and thus encourage the stress anisotropy in soils at that location.

Pictures taken at four different elapsed times by means of high-speed CCD camera are shown in Fig. 5 for case 8. It is seen that the boundary between the mound and the foundation ground bends into the foundation soils with time. Colored sand markers displace accordingly. Vertical and horizontal strains in the upper and middle layers of the foundation deposits are deduced from the pictures by high-speed CCD camera, and are plotted against time in Fig. 6. Solid lines indicate strains observed in the upper layer, and the dotted lines denote strains in the middle layer. Vertical compressive strains develop from the beginning of earthquake loading, and cease to increase when the shaking stops. These are accompanied by simultaneous development of horizontal tensile strains. The vertical compressive strains at the end of the shaking are 12 % and 35 % in the upper and middle layers respectively. As explained earlier in Fig. 4, soils in the middle or upper part of the foundation ground beneath the caisson do not undergo liquefaction during shaking, though the undrained cumulative shear deformation mechanism does become operational to cause significant axial deformations.

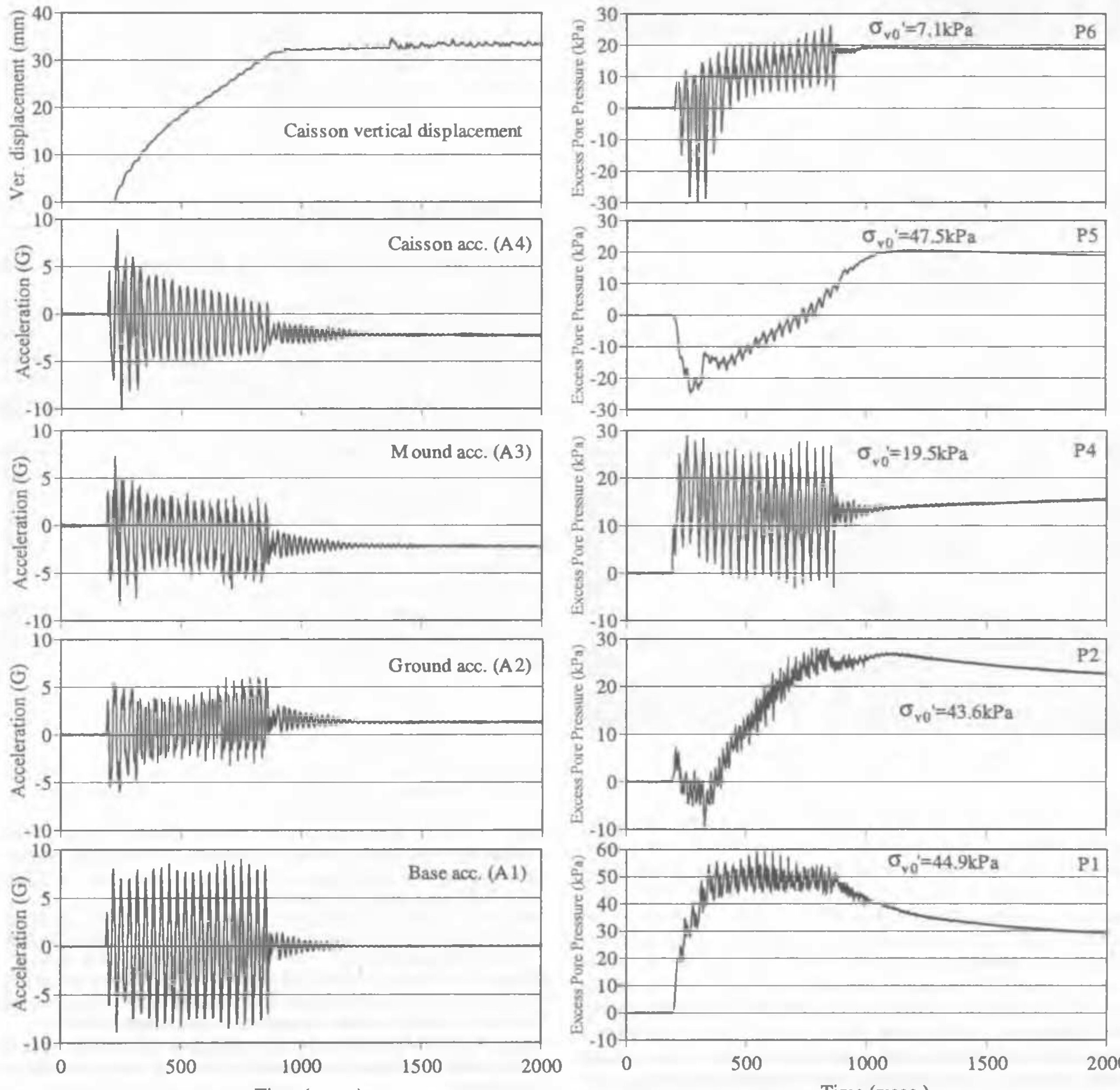

Figure 4. Time histories of accelerations, excess pore pressures and displacement of caisson (Case 8).

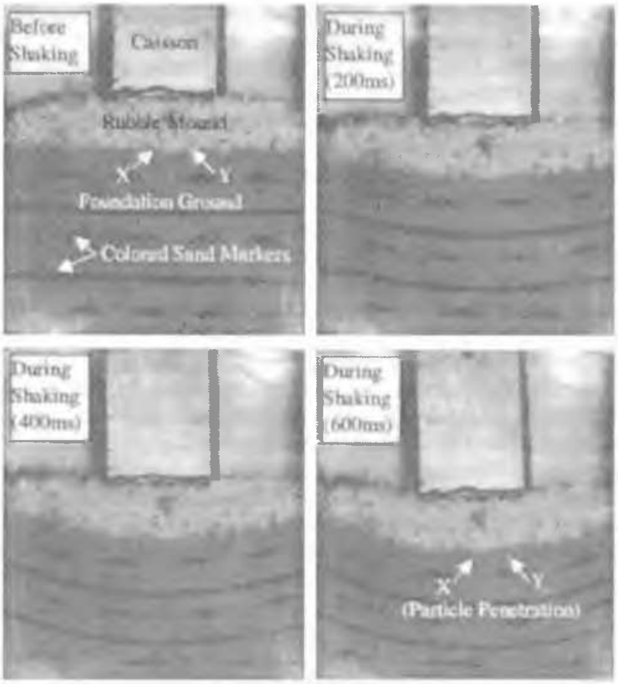

Figure 5. Deformation of mound and foundation ground observed using high-speed CCD camera (Case 8).

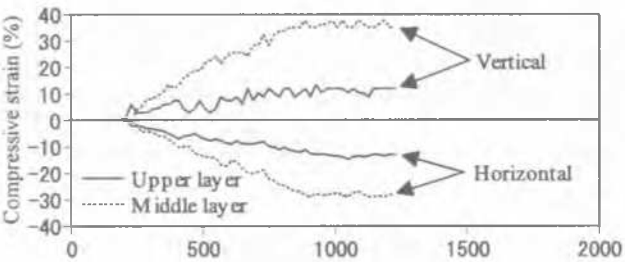

Figure 6. Time histories of strains in the upper and middle layers of the foundation ground (Case 8).

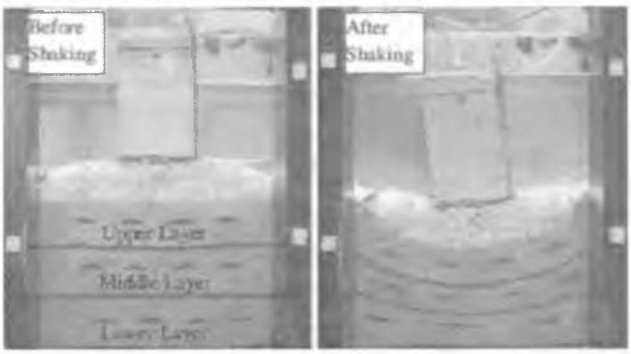

Figure 7. Deformation of caisson and model ground (Case 8).

Photographs of model ground taken before and after the earthquake loading are shown in Fig. 7. Vertical compressive strains are measured from these pictures for the upper, middle and lower layers, and are listed in Table 2 for all experimental cases. It is interesting to note that the largest strain was observed in the middle layer in experiments with loose foundation deposits (Dr<40%), whereas the largest strains occurred in the lower layer in cases for medium dense deposits (Dr>40%). Recalling the results of cyclic torsional shear tests by Tanaka (Fig.1) and the distribution of initial shear stress ratio in Fig.2, the undrained cumulative shear deformation mechanism is suppressed to some extent in soils at the shallow depths beneath the main part of composite breakwater, where large initial shear stress is induced by the weight of the caisson and mound.

One may observe the penetration of coarse mound rubbles into the foundation soils after the earthquake loading in Figs. 5 and 7. Particles dispersed into the foundation soils were collected and the dry mass was measured for the purpose of evaluating the influence of particle dispersion onto the caisson settlement. Settlements due to dispersion are divided by the settlements at the caisson top, and are shown as "penetration ratio of mound" in Table 1. It can be noted that the larger the contrast in particle sizes between the mound and foundation deposits, the larger the penetration ratio becomes. In this particular series of experiments, settlement caused by dispersion amounted to about 20% of total settlement for gravel mound cases, while the ratio was several percent for cases with a sandy mound. In other words, settlements due to dispersion approximately equaled the particle sizes.

Table 2 Compressive strain of foundation ground

Case No.	Upper layer (%)	Middle layer (%)	Lower layer (%)	Dr (%)
1	3.5	12.0	26.0	47
2	7.2	15.0	21.0	44
3	14.7	31.7	10.1	31
4	8.7	59.0	21.0	15
5	23.2	45.5	27.5	30
6	0.7	12.8	20.7	58
7	16.2	39.3	31.7	37
8	13.1	43.6	37.2	22
9	21.4	50.1	33.7	23

4 CONCLUDING REMARKS

The principal results obtained in this study may be summarized as follows:

(1) Foundation ground just beneath the main part of a composite breakwater may undergo large axial deformation (vertical compression associated with horizontal extension) during ground shaking, due to the undrained cumulative shear deformation mechanism, which becomes operational once effective stresses reach phase transformation states.

(2) The vertical compressive strains in the middle and lower (deep) layers were larger than those in the upper (shallow) layers. This is a consequence of the following two factors; (i) marked decrease in the effective confining stress at the deeper soil depth during shaking. (N.B. The initial shear stress ratio in deep layers was smaller than that in shallow layers.) (ii) Marked increase in the amplitude of cyclic shear stress at the deeper soil depth.

(3) The penetration of the mound rubble into the fine-grained foundation soil amounted to a settlement that was approximately equal to the size of rubble used.

REFERENCES

Iai, S., Ichii, K., Liu, H. L. and Morita, T. 1998. Effective stress analyses of port structures. *Special Issue of Soils and Foundations* No.2: 97-114. Japanese Geotechnical Society.

Peiris, L. M. N., Madabhushi, S. P. G. and Schofield, A. N. 1998. Dynamic behaviour of gravel embankments on loose saturated sand foundatiuons. *Proceedings of International Conference CENTRIFUGE 98* Vol.1: 263-270. Rotterdam: Balkema.

Sekiguchi, H., Kita, K., Hashimoto, K. and Katsui, H. 1996a. Deformation of composite breakwaters due to ground shaking. *Special Issue of Soils and Foundations* No.1: 169-177. Japanese Geotechnical Society.

Sekiguchi, H., Tanaka, K., Sassa, S. and Kita, K. 1996b. Performance of undrained cyclic torsional shearing of saturated sands. *Proceedings of the 1st JSPS-NUS Seminar on Integrated Engineering*: 50-59.

Tanaka, K. 1996. *Performance of undrained cyclic torsional shearing of anisotropic consolidated sands.* Master Thesis, Kyoto University (in Japanese).